NACA RM E52L22a

NACA

RESEARCH MEMORANDUM

DESIGN AND TEST OF MIXED-FLOW IMPELLERS

III - DESIGN AND EXPERIMENTAL RESULTS FOR IMPELLER MODEL MFI-2A AND COMPARISON WITH IMPELLER MODEL MFI-1A

By Joseph T. Hamrick, Walter M. Osborn, and William L. Beede

Lewis Flight Propulsion Laboratory
Cleveland, Ohio

NATIONAL ADVISORY COMMITTEE
FOR AERONAUTICS

WASHINGTON

March 10, 1953
Declassified January 20, 1958

NATIONAL ADVISORY COMMITTEE FOR AERONAUTICS

RESEARCH MEMORANDUM

DESIGN AND TEST OF MIXED-FLOW IMPELLERS

III - DESIGN AND EXPERIMENTAL RESULTS FOR IMPELLER MODEL MFI-2A AND COMPARISON WITH IMPELLER MODEL MFI-1A

By Joseph T. Hamrick, Walter M. Osborn, and William L. Beede

SUMMARY

A mixed-flow impeller was designed to give a prescribed blade-surface velocity distribution at mean blade height for a given hub-shroud profile. The blade shape at mean blade height, which was produced by the prescribed velocity distribution, was extended by means of radial lines to form the composite blade shape from hub to shroud. The resulting blade was relatively thick; therefore, it was necessary to retain the inverse blade taper which resulted from extension of the radial lines in order to prevent merging or near merging of the separate blades near the hub. For the first test version of the impeller, designated the MFI-2A, the blade height was arbitrarily made greater than that for the basic impeller (the MFI-2) to allow for viscous effects.

At design equivalent speed of 1400 feet per second the peak pressure ratio and maximum adiabatic efficiency were 3.95 and 79 percent, respectively. The adiabatic efficiency of the MFI-2A is four points lower than that for impeller model MFI-1A, but because of the higher slip factor for the MFI-2A, the pressure ratios are approximately equal.

The procedures followed in the design of the MFI-1A and MFI-2A were, in general, the same; and, although the prescribed initial condition resulted in geometrical configurations that were quite dissimilar, the resulting performance characteristics compare favorably with designs for which considerable development work has been necessary.

INTRODUCTION

Impeller model MFI-2 is the second in a series of mixed-flow impellers being designed and experimentally investigated at the NACA Lewis laboratory. The purpose of the design and test of this series of impellers is to develop a reliable design procedure which will eliminate the large amount of experimental development work which has been necessary in the past.

The design procedure followed in the design of the MFI-2 impeller is, in general, the same as that used to design the MFI-1 of reference 1. Briefly, the method is as follows: design of the impeller blade to produce a given velocity distribution at mean blade height for a given hub-shroud profile, formation of the composite blade by passing radial lines through the blade profile at mean blade height, and analysis of the flow through the passage between blades to determine the velocity distribution at other than mean blade height.

For each impeller the design blade height was arbitrarily increased to provide for investigation of boundary-layer and viscous effects in the latter part of the flow passage. This blade height will be decreased to the design value in successive steps in order to determine the optimum allowance for viscous effects for each impeller.

The MFI-2 is somewhat different from the MFI-1 in that the blades are thicker, they are tapered in the opposite direction (inverse taper), and the ratio of blade height to passage width is greater. In addition, the blade camber-line shape of the MFI-2 is less conventional than that of the MFI-1. In the design of the MFI-2 the same general design criteria as for the MFI-1 were followed, namely, gradual loading and unloading of the blades, avoidance of decelerating flow wherever possible, and limitation to a maximum relative velocity ratio Q (ratio of velocity relative to impeller to velocity of sound at inlet stagnation conditions) of approximately 1.2. In addition, an effort was made in this design to reduce secondary-flow effects by designing for a high ratio of blade height to passage width.

The experimental test results of the first test version of the MFI-2, designated the MFI-2A, are reported herein; and a comparison is made of the over-all performances of the MFI-1A and the MFI-2A.

SYMBOLS

The following symbols are used in this report:

h blade height perpendicular to mean blade-height line (fig. 1)

L ratio of distance along streamline or mean line from inlet to total distance along streamline or mean line from inlet to outlet

Q ratio of velocity relative to impeller to velocity of sound at inlet stagnation conditions

q velocity relative to impeller, ft/sec

U actual impeller speed at 7.00-in. radius (outlet mean line), ft/sec

W total compressor flow rate, lb/sec

β blade angle (fig. 4, negative for backward-curved blades)

δ ratio of total pressure at inlet to NACA standard sea-level pressure (29.92 in. Hg abs)

θ ratio of inlet stagnation temperature to NACA standard sea-level temperature, 518.4° R

φ angle between projection of center line of blade-inlet radial section and projection of center line of any other blade radial section on plane perpendicular to axis of rotation (fig. 5), deg

ω angular velocity of impeller, radians/sec

DESIGN AND THEORETICAL ANALYSIS

Design Procedure

The procedure followed in the design of impeller model MFI-2 is the same as that given in reference 1 for impeller model MFI-1, for which references 2 and 3 were utilized. The inlet and exit annuli and shroud and diffuser shapes for the MFI-2 are identical with those for the MFI-1. The basic differences in the MFI-1 and MFI-2 designs are brought out in the following discussion.

Hub-shroud shape. - The hub-shroud shape for the MFI-2 with blade-height lines and mean line is shown in figure 1. Starting with the shroud shape for the MFI-1, the location of the mean line was chosen so as to produce a blade height greater than that for the MFI-1 while maintaining equal inlet and exit blade heights for the two impellers. Blade-height lines h were then drawn perpendicular to and symmetrical about the mean line with the shroud used as one extremity. The opposite extremities determined the hub contour. The requirement for relatively thin blades dictated to a large extent the height of the h lines for the MFI-1. The restriction to relatively thin blades was not made for the MFI-2 except at the inlet and the exit. A specific attempt was made to obtain a relatively high ratio of blade height to passage width for the following reason: An increase in blade height reduces both the blade loading (static-pressure difference between blade driving surface and trailing surface) and tangential pressure gradient; therefore, both flow decelerations due to unloading the blades and circumferential secondary flows due to tangential pressure gradients may theoretically be

reduced by increasing the blade height. Also, the proportion of the losses due to interaction of blade and shroud boundary layers may be reduced. The blade loading may also be reduced by increasing the number of blades, but the tangential pressure gradient is not reduced. An increase in the ratio of blade height to passage width for the MFI-2 over that for the MFI-1 was obtained as shown in figure 2.

Velocity distribution. - The prescribed velocity distribution is given in figure 3. It was expected that for this impeller the maximum weight flow would be near the theoretical maximum of 14.5 pounds per second for the MFI-1; therefore the design weight flow was set at 13 pounds per second in an attempt to keep well below the choke flow point. Because of the reduced weight flow, the exit relative velocity is approximately equal to that at the inlet instead of being higher as it was for the MFI-1. The blade loading as previously defined, which is determined by the velocity distribution, is lower for the MFI-2 because of the higher blade height and lower design weight flow. In addition, the loading and unloading of this blade at entrance and exit, respectively, are more gradual.

Blade shape. - The blade shape at the mean line which resulted from the prescribed velocity distribution is shown in figure 4. The original blade shape was modified as shown in order to produce a more desirable velocity distribution near the shroud and increase the maximum flow rate. For the MFI-1 impeller the hub instead of the blade was modified to produce these effects.

The composite blade shape was formed by passing radial lines through the final blade profile (fig. 4), which lies on the mean-line surface of revolution. Formation of the blade in this manner resulted in inverse taper, which can be seen in figure 5. For blades as thick as this it was necessary to retain the inverse taper in order to prevent merging or near merging of the separate blades at the hub. The use of inverse taper is in closer conformity with the assumption made in the use of reference 2.

Design Data

In the design of the impeller, the following specifications and limitations were used:

Impeller outlet mean-line speed (7.00 in. outlet mean radius), ft/sec	1400
Design flow rate, lb/sec	13.00
Slip factor (based on blade outlet angle equal to zero)	1.00
Prerotation	0
Axial inlet velocity, ft/sec	430
Relative velocity q at mean inlet radius, ft/sec	772
Limiting relative velocity ratio	1.2
Number of blades	20
Exit cone angle (approximate), deg	30

The geometric coordinates for the MFI-2 are given in table I.

Theoretical Analysis

An analysis of the flow at 13.0 pounds per second was made by the method of reference 3. The analysis in the meridional plane is shown in figure 6, and the blade-surface velocity distribution is shown in figure 7.

Streamlines. - The flow streamlines and normals are shown in figure 6(a). The solution of the flow in the meridional plane was made along the normals shown for 20 stream tubes in the first two thirds of the impeller passage and for 10 stream tubes thereafter with equal weight flows through the stream tubes. Only 10 stream tubes are shown in figure 6(a).

Velocity distribution. - Lines of constant relative velocity ratio Q in the meridional plane are shown in figure 6(b). The flow along the hub decelerates to point A and then accelerates to point B, from which point it decelerates to the exit. There were no decelerations in flow along the hub of the MFI-1 except for a negligible amount near the exit. In this respect, the MFI-1 may be superior to the MFI-2. The blade-surface velocity distribution is given in figure 7 for six stream tubes from hub to shroud. Velocity gradients in the direction of flow can be more easily observed in this figure. The deceleration near the inlet for stream tubes 0, 4, and 8 (figs. 7(a), 7(b), and 7(c), respectively) resulted from the increase in through-flow area required to give a relative velocity ratio less than 1.2 at the shroud.

Meridional pressure distribution. - Lines of constant static-pressure ratio (ratio of static pressure to inlet total pressure) are shown in figure 6(c). The ratio decreases from hub to shroud near the inlet. The static-pressure ratio ahead of the impeller with uniform velocity across the annulus is 0.90. The pressure ratio at the streamline for 30-percent flow is below 0.90, with the ratio decreasing rapidly toward the shroud. The drop in pressure ratio to well below 0.90 near the shroud is due to the large effects of the small area reduction upon the near-sonic relative velocities entering the blade row. From the streamline at 30-percent flow toward the hub, the pressure ratio is higher than 0.90, which indicates sudden energy addition due to positive angle of attack at the inlet. The positive angle of attack is caused by slowing down of the air along the inner annulus wall due to hub-shroud curvature.

Angle of attack. - The angle of attack is defined as the angle between the average flow direction of the air at the inlet and the blade camber line, with flow directed at the driving face of the blade forming a positive angle of attack. An approximate angle of attack was determined as follows: Each meridional stream tube at the inlet was extended a short distance into the upstream annulus in the axial direction. The upstream axial velocity corresponding to the weight flow for each stream tube was used to compute the average angle of entry into the impeller. The angle made with the blade camber line is shown in figure 8. Sweeping the blades back from hub to tip would provide a more nearly constant angle of attack across the inlet and would allow larger increases in weight flow above design weight flow before negative angles of attack are encountered.

Maximum weight flow. - In the theoretical analysis, choking occurred at the first normal for the design speed (outlet mean-line speed of 1400 ft/sec). With choking at the inlet, the theoretical calculations are subject to excessive error due to failure of the air to follow the direction of the blade. A discussion of this effect is given in reference 4. The calculated maximum flow at the first normal is 13.65 pounds per second and at the third normal is 15.44 pounds per second. From the performance of the MFI-1A of reference 4, it was expected that the maximum weight flow would fall between these two values.

Modified Impeller MFI-2A

The blade height of the MFI-2 impeller was increased to provide for an investigation of viscous effects. The increase was made the same as that for the MFI-1A so that the same shroud could be used for both impellers. The resulting impeller was designated the MFI-2A. The 74-percent increase in blade height at the outlet is probably too great for the MFI-2A as compared with the MFI-1A, inasmuch as the design weight flow for the

MFI-2A is lower. In addition, it is expected that reducing the blade height of the MFI-2A to the design value will be less critical than for the MFI-1A because of the higher initial blade height of the MFI-2A except at inlet and exit. A front view of the MFI-2A is shown in figure 5 and a photograph is shown in figure 9.

EXPERIMENTAL RESULTS

Apparatus, Instrumentation, and Procedure

The apparatus and instrumentation for the MFI-2A are identical with that for the MFI-1A of reference 4. The inlet total temperature and pressure were measured in a depression tank ahead of the impeller inlet, and the outlet total temperature and pressure were measured at a radius $1\frac{1}{2}$ times that of the impeller (10.5 in.) in the vaneless diffuser. The actual distance from the impeller tip was $5\frac{1}{2}$ inches. The test and computation procedures are the same as those used in reference 4.

RESULTS AND DISCUSSION

The over-all performance of the MFI-2A impeller is shown in figure 10. The peak pressure ratio and maximum adiabatic efficiency at the design equivalent speed of 1400 feet per second were 3.95 and 79 percent, respectively. A comparison of this performance with that of the MFI-1A shows that for these versions of the basic impellers the MFI-1A is superior. Comparisons of pressure ratio, efficiency, slip factor, and weight-flow range for the two impellers are shown in figure 11. The performance in each case may be improved as the blade height is reduced toward the design value.

Over-all pressure ratio. - Maximum pressure ratio over the range of exit mean-line speeds is given in figure 11(a). The MFI-2A has a slightly lower pressure ratio above a mean-line speed of 900 feet per second. Inasmuch as the MFI-2A has a higher slip factor, its pressure ratio should be higher. However, a lower efficiency for the MFI-2A offsets the difference in slip factor.

Efficiency. - Maximum efficiency over the speed range is shown in figure 11(b). The efficiency over the speed range is generally lower for the MFI-2A than for the MFI-1A and at design speed is four points lower.

Slip factor. - The slip factor at maximum efficiency is plotted against outlet mean-line speed in figure 11(c). This slip factor is based

on an average inlet-air temperature, a mass-flow-average outlet temperature, and an actual impeller speed as computed at a root-mean-square radius of 7.19 inches. If the disk friction losses between the impeller and shroud can be neglected, this value is equal to approximately the tangential velocity of the air divided by the blade speed at the outlet.

It was expected that the slip factor for the MFI-2A would be greater than or at least equal to that obtained for straight blades by the relaxation solutions of reference 5. The value of 0.91 for 1400 feet per second, however, fell below the theoretical value of 0.95 of reference 5. A reduction in slip factor could have arisen in the following manner (with the data of ref. 6 used as a basis): If separation occurred along the trailing face of the blade near the outlet, as it may well have for the efficiency obtained, the flow would have followed a path more nearly parallel to the driving face of the blade which is backward curved (fig. 4). Altering the flow direction in this manner would reduce the slip factor.

Weight-flow range. - The weight-flow range for the two impellers is shown in figure 11(d). The maximum weight flow of 14.9 pounds at 1400 feet per second for the MFI-2A falls within the range of 13.65 to 15.45 pounds per second obtained by the theoretical analysis. The extent of the flow range for the two impellers is about the same.

Static-pressure ratios. - The theoretical and experimental static-pressure ratios at design speed (1400 ft/sec) and weight flow of 13 pounds per second are given in figure 12 for flow along the shroud. The experimental and theoretical static pressures agree very well just upstream of the inlet; therefore, the theoretical and experimental angles of attack near the shroud should agree. The rapid drop in pressure just inside the inlet for the theoretical case is caused by an increase in relative velocity to values above sonic. The drop in experimental static pressure at L equal to approximately 0.30 may be due to flow separation. The tendency to separate in this region may be increased because of the increased through-flow area of this version of the impeller.

Relative velocity ratio. - The static pressure along the shroud was used to determine the average relative velocity at the shroud for estimated values of relative internal efficiency as defined in reference 6. The estimates were based upon the data of reference 6. In figure 13 the theoretical, average, relative velocity ratio is compared with the experimental for two estimated values of internal efficiency. The drop in static pressure at L equal to approximately 0.30 is reflected in the velocity by an increase in velocity at that point. It is possible that the deceleration of flow along the shroud was too large and resulted in separation at 1400 feet per second. A comparison of the relative velocity ratio at maximum efficiency for varying impeller speeds (fig. 14)

shows that the velocity increase at L equal to approximately 0.30 becomes smaller with decreasing speed. Estimates of internal efficiency used in computing velocities were chosen to agree with the over-all efficiency for each speed and were assumed constant along the flow path at each speed. The internal efficiencies for the impeller of reference 6 varied along the flow path. However, the change in the circumferential average of the relative internal efficiency was small for the weight flow corresponding to maximum over-all efficiency.

The agreement between the theoretical and the experimental velocity at the exit in figure 13 indicates that at least sufficient allowance for viscous effects was made at the impeller outlet. However, an improper increase prior to the outlet may have produced losses which resulted in the agreement. The procedures followed in the design of the MFI-1A and MFI-2A were, in general, the same; and, although the prescribed initial condition resulted in geometrical configurations that were quite dissimilar, the resulting performance characteristics compare favorably with designs for which considerable development work has been necessary.

Concluding remarks. - The impellers have been compared in this report because they were designed by the same procedure and not because they give direct comparisons of factors such as the ratio of blade height to passage width, or blade loading. For example, the lower efficiency of the MFI-2A could have been due to greater deceleration rates near the hub inlet and along the blade trailing face near the outlet. An important feature in this comparison is the arbitrary increase in blade design height which may have been less favorable for the MFI-2A because of the higher deceleration rates. Whether or not this is true may be brought out in the experimental investigations with reduced blade height. In the use of this design method the need for information as to the severity of the velocity gradients that may be tolerated is apparent. In addition, some knowledge of the effect of increased blade loading upon shroud and blade boundary-layer interaction is desirable.

SUMMARY OF RESULTS

A mixed-flow impeller was designed to give a prescribed blade-surface velocity distribution at mean blade height for a given hub-shroud profile. The blade shape at mean blade height which was produced by the prescribed velocity distribution was extended by means of radial lines to form the composite blade shape from hub to shroud. The resulting blade was relatively thick; therefore it was necessary to retain the inverse blade taper which resulted from extension of the radial lines in order to prevent merging or near merging of the separate blades near the hub. For the first test version of the impeller, designated the MFI-2A, the blade height was arbitrarily increased to provide for investigation of viscous effects. Experimental investigation of the impeller model MFI-2A and comparison with impeller model MFI-1A gave the following results:

1. The peak pressure ratio and maximum adiabatic efficiency at the design equivalent speed of 1400 feet per second were 3.95 and 79 percent, respectively.

2. At design speed the arbitrary increase in blade height at exit was apparently sufficient to allow for the decrease in effective flow area caused by viscous effects. However, an improper increase prior to the exit may have caused separation losses which produced this result.

3. The adiabatic efficiency for the MFI-1A is 4 points higher than for the MFI-2A at design speed; but because of the higher slip factor for the MFI-2A, the pressure ratios are approximately equal.

4. The extent of the flow range for the two impellers is approximately the same.

Lewis Flight Propulsion Laboratory
National Advisory Committee for Aeronautics
Cleveland, Ohio

REFERENCES

1. Osborn, Walter M., and Hamrick, Joseph T.: Design and Test of Mixed-Flow Impellers. I - Aerodynamic Design Procedure. NACA RM E52E05, 1952.

2. Stanitz, John D.: Approximate Design Method for High-Solidity Blade Elements in Compressors and Turbines. NACA TN 2408, 1951.

3. Hamrick, Joseph T., Ginsburg, Ambrose, and Osborn, Walter M.: Method of Analysis for Compressible Flow through Mixed-Flow Centrifugal Impellers of Arbitrary Design. NACA Rep. 1082, 1952. (Supersedes NACA TN 2165.)

4. Withee, Joseph R., Jr., and Beede, William L.: Design and Test of Mixed-Flow Impellers. II - Experimental Results with a Model MFI-1A Impeller. NACA RM E52E22, 1952.

5. Stanitz, John D., and Ellis, Gaylord O.: Two-Dimensional Compressible Flow in Centrifugal Compressors with Straight Blades. NACA Rep. 954, 1950.

6. Prian, Vasily D., and Michel, Donald J.: An Analysis of Flow in Rotating Passage of Large Radial-Inlet Centrifugal Compressor at Tip Speed of 700 Feet Per Second. NACA TN 2584, 1951.

TABLE I. - GEOMETRIC COORDINATES FOR USE IN CONSTRUCTING MFI-2 AND MFI-2A IMPELLERS

[Number of blades, 20; material, aluminum alloy (14S-T6).]

Axial depth, in.	Blade thickness at hub, in.	Blade thickness at mean line (MFI-2), in.	Blade thickness at shroud (MFI-2A), in.	Hub radius, in.	Mean-line radius (MFI-2), in.	Shroud radius (MFI-2), in.	Shroud radius (MFI-2A), in.	Angle φ
0	0.092	0.092	0.092	1.680	3.200	4.725	4.725	0
.100	.112	.112	.112	1.683	3.203	-----	4.743	3° 14'
.200	.112	.127	.142	1.690	3.210	4.736	4.763	4° 18'
.400	.112	.154	.196	1.705	3.230	4.758	4.792	8° 18'
.600	.112	.182	.252	1.730	3.265	4.789	4.819	11° 54'
.800	.114	.211	.310	1.762	3.310	4.823	4.863	14° 57'
1.000	.134	.251	.366	1.805	3.370	4.868	4.915	17° 36'
1.400	.185	.338	.483	1.932	3.525	4.973	5.040	21° 30'
1.800	.251	.440	.617	2.120	3.710	5.098	5.200	23° 58'
2.200	.346	.575	.787	2.365	3.930	5.247	5.380	25° 12'
2.600	.426	.674	.904	2.632	4.160	5.417	5.580	25° 24'
3.000	.481	.722	.945	2.940	4.415	5.611	5.782	24° 43'
3.400	.530	.758	.970	3.285	4.695	5.808	6.006	23° 18'
3.800	.565	.776	.962	3.660	5.020	6.005	6.228	21° 13'
4.200	.580	.762	.913	4.098	5.385	6.203	6.454	18° 49'
4.600	.575	.709	.824	4.660	5.750	6.399	6.680	16° 34'
5.000	.545	.628	.711	5.295	6.100	6.598	6.902	14° 48'
5.400	.453	.496	.551	5.852	6.410	6.795	7.128	13° 37'
5.800	.275	.293	.323	6.275	6.680	6.992	7.352	12° 58'
6.200	.123	.129	.141	6.618	6.930	7.190	7.580	12° 52'
6.298	.096	.100	.109	6.700	6.994	7.239	7.636	12° 52'

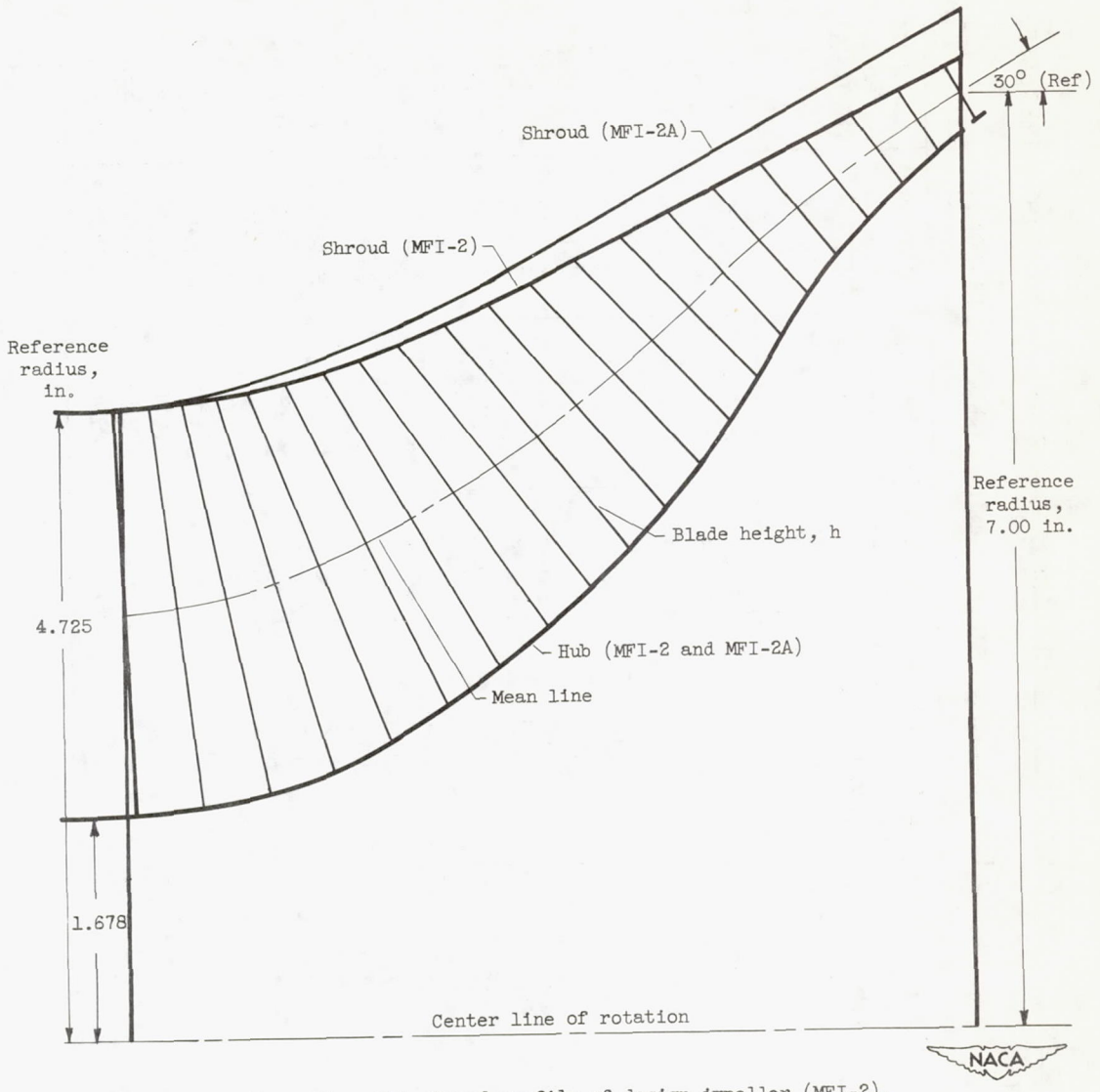

Figure 1. - Hub-shroud profile of design impeller (MFI-2).

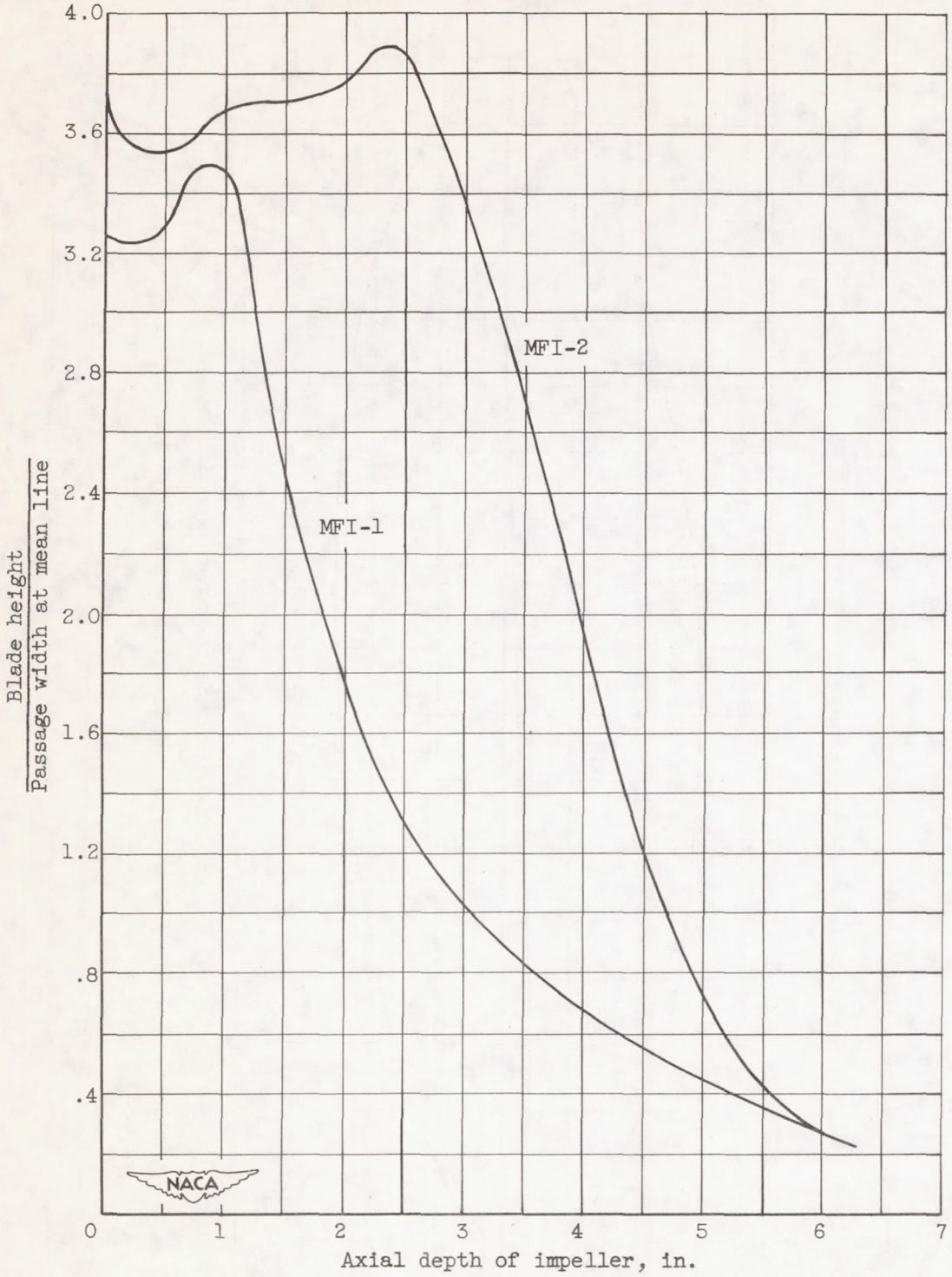

Figure 2. - Comparison of blade height with passage width for MFI-1 and MFI-2 impellers.

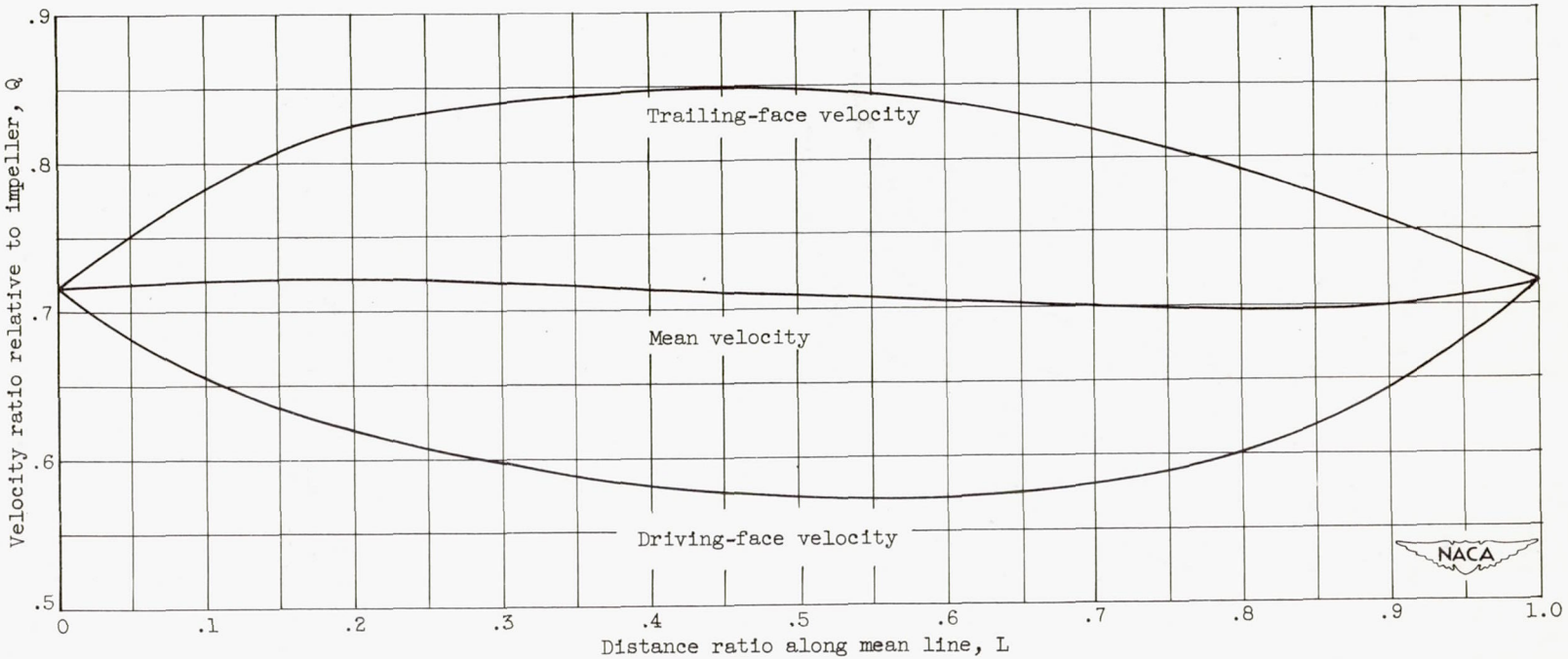

Figure 3. - Prescribed velocity diagram for design impeller (MFI-2).

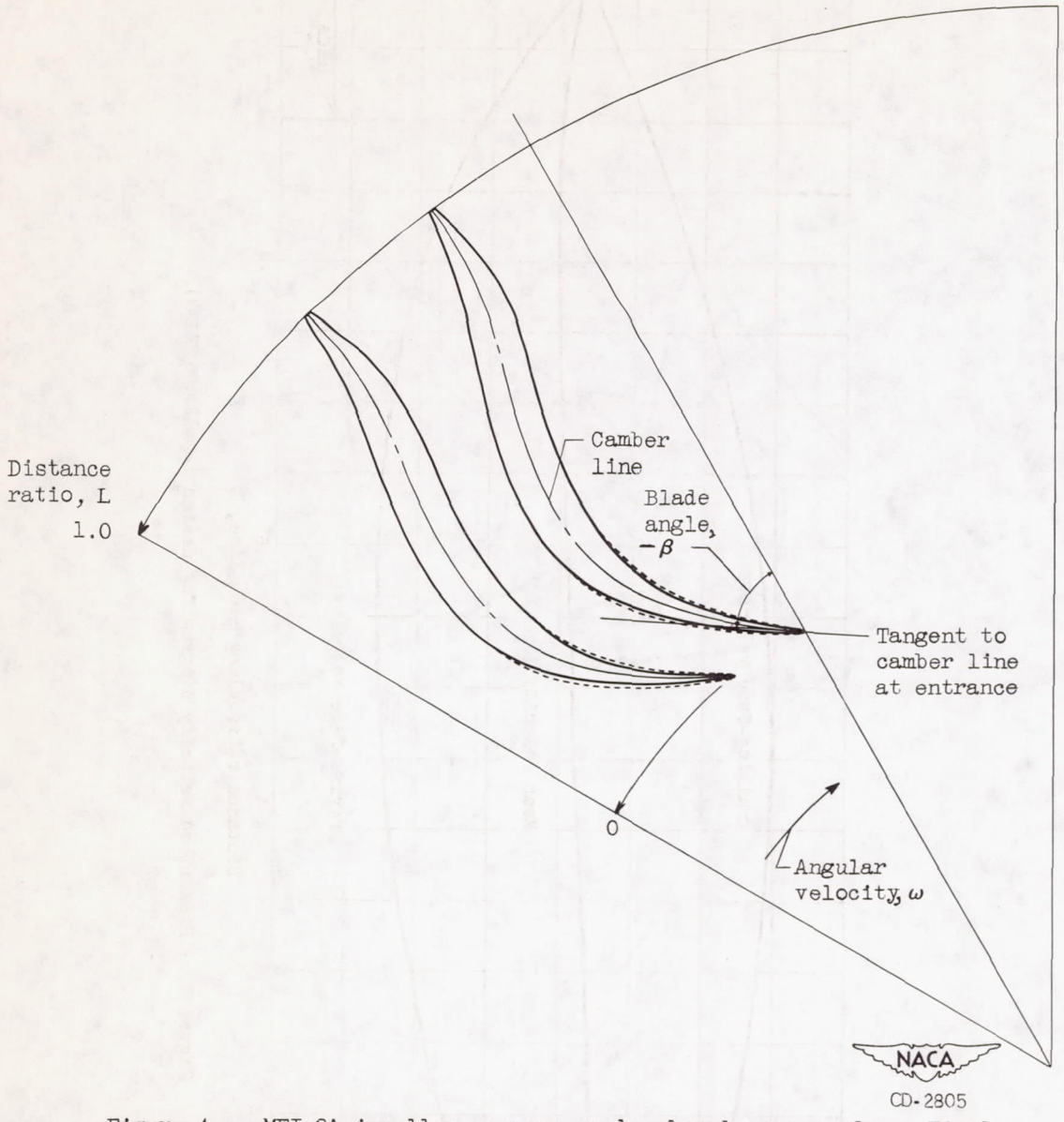

Figure 4. - MFI-2A impeller passage on developed cone surface. Final blade profile at mean line is shown by solid lines. Portion of original blade profile which was modified is shown by broken lines.

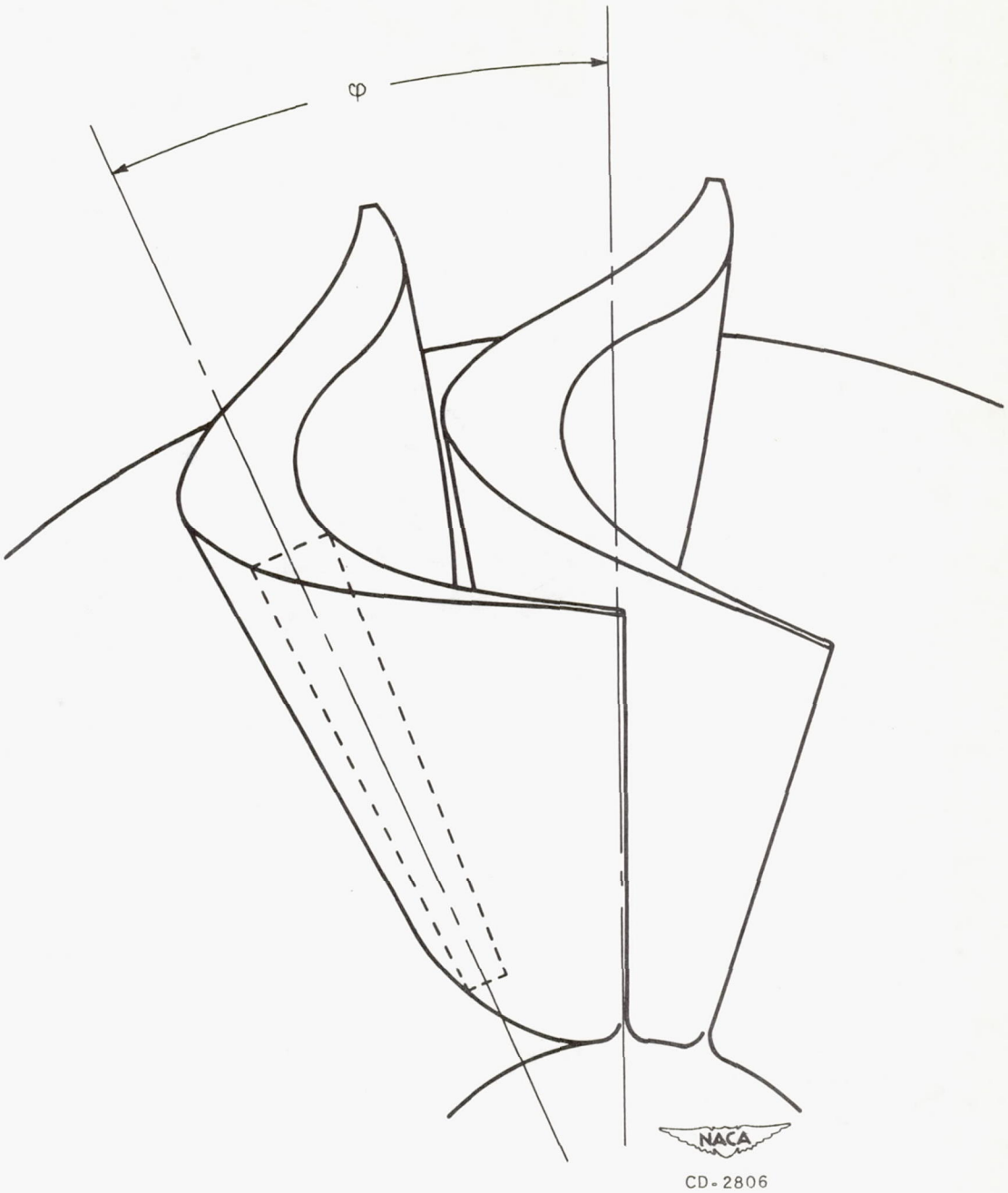

Figure 5. - Front view of MFI-2A impeller blades and passage.

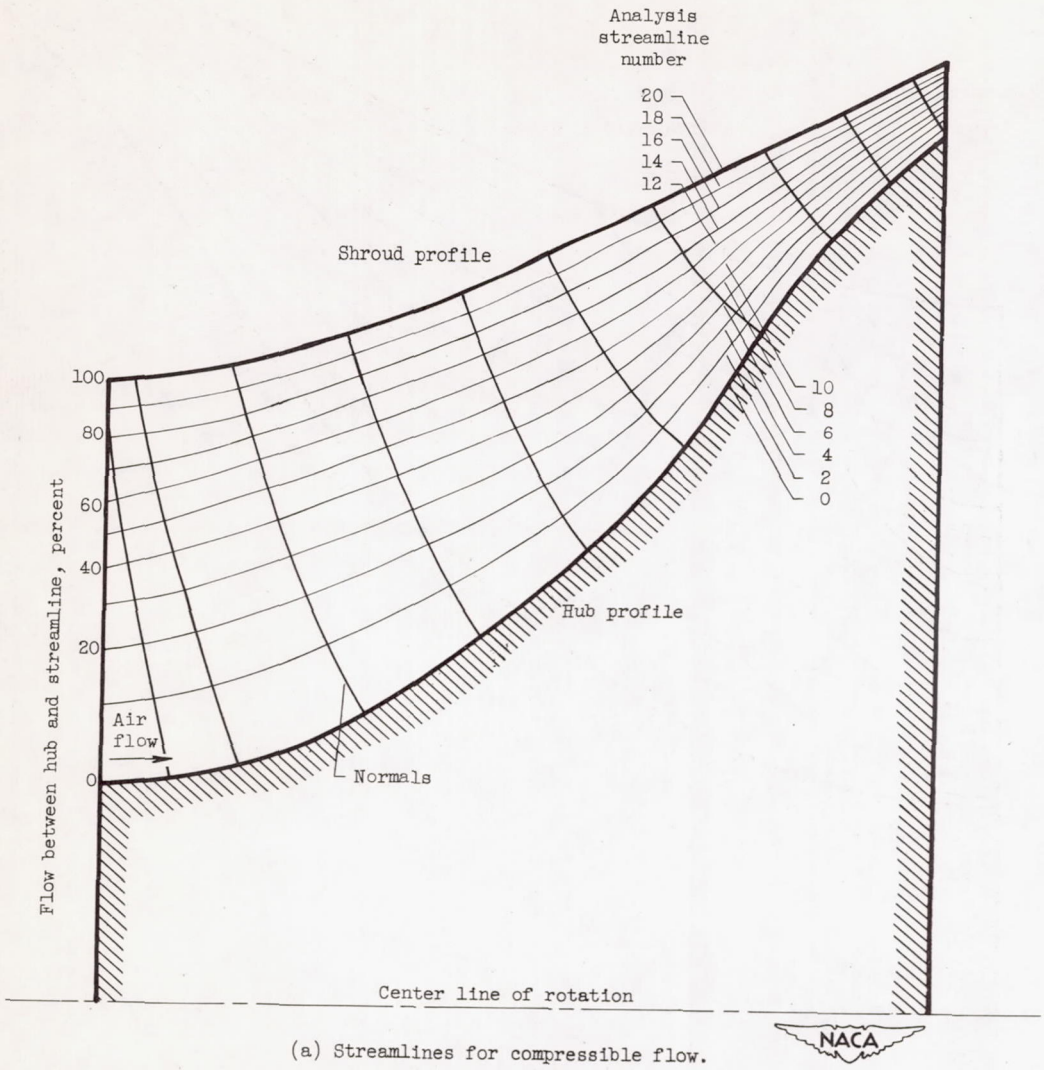

(a) Streamlines for compressible flow.

Figure 6. - Flow analysis for design impeller (MFI-2) in meridional plane. Weight flow, 13.0 pounds per second; outlet mean-line speed, 1400 feet per second.

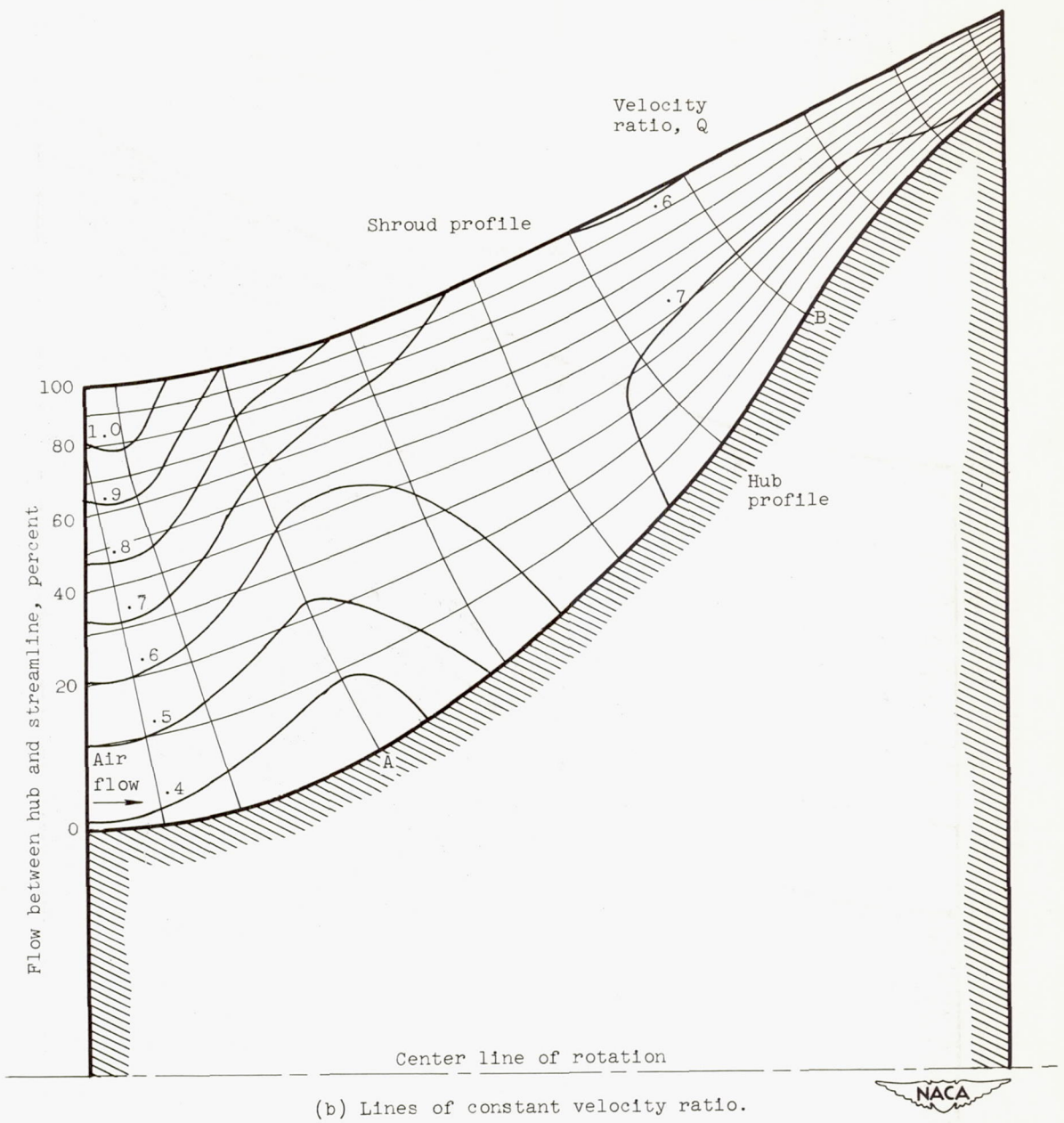

(b) Lines of constant velocity ratio.

Figure 6. - Continued. Flow analysis for design impeller (MFI-2) in meridional plane. Weight flow, 13.0 pounds per second; outlet mean-line speed, 1400 feet per second.

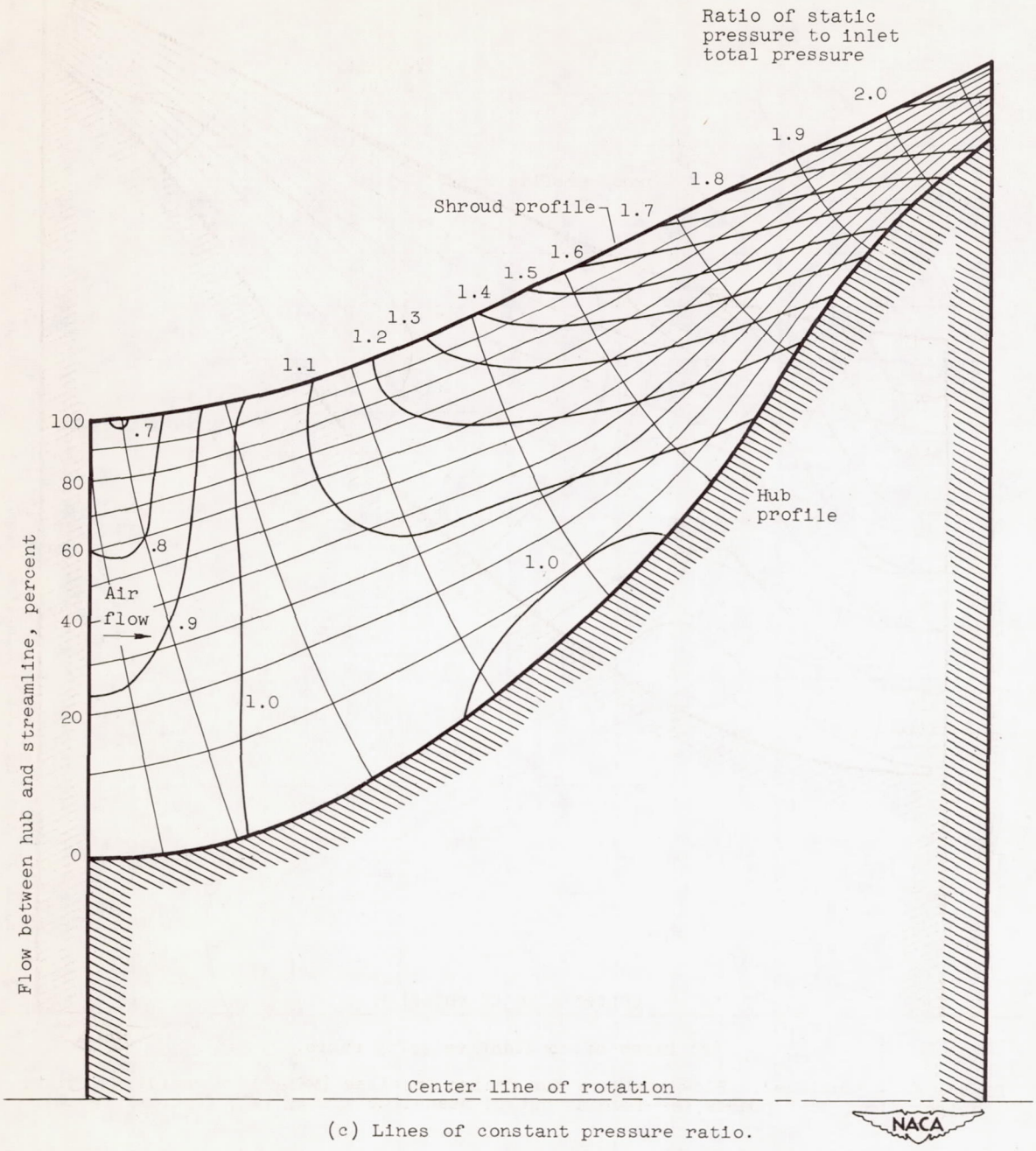

(c) Lines of constant pressure ratio.

Figure 6. - Concluded. Flow analysis for design impeller (MFI-2) in meridional plane. Weight flow, 13.0 pounds per second; outlet mean-line speed, 1400 feet per second.

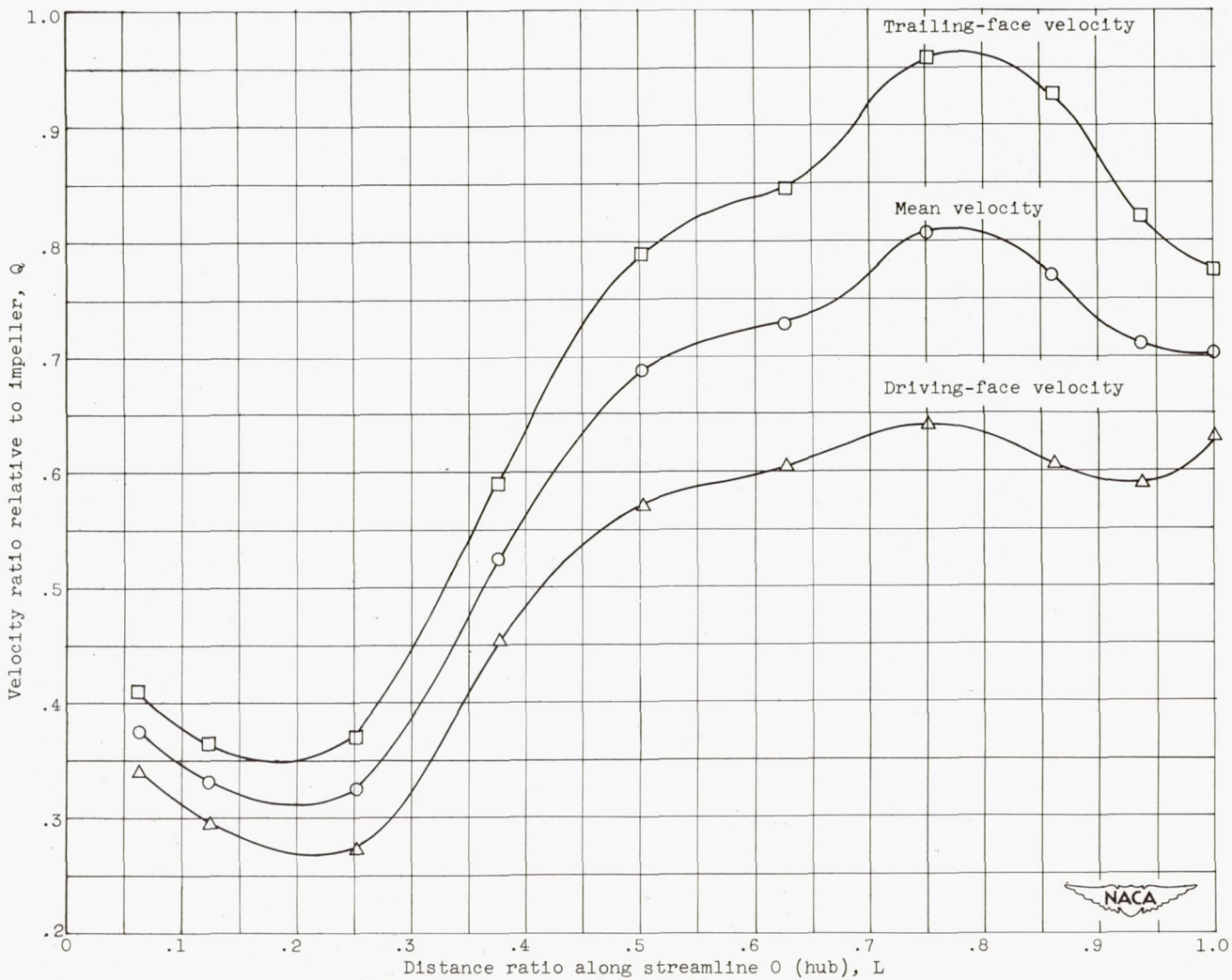

(a) Blade-to-blade velocity distribution along streamline 0 (hub).

Figure 7. - Flow analysis in blade-to-blade plane for design impeller (MFI-2). Weight flow, 13.0 pounds per second; outlet mean-line speed, 1400 feet per second.

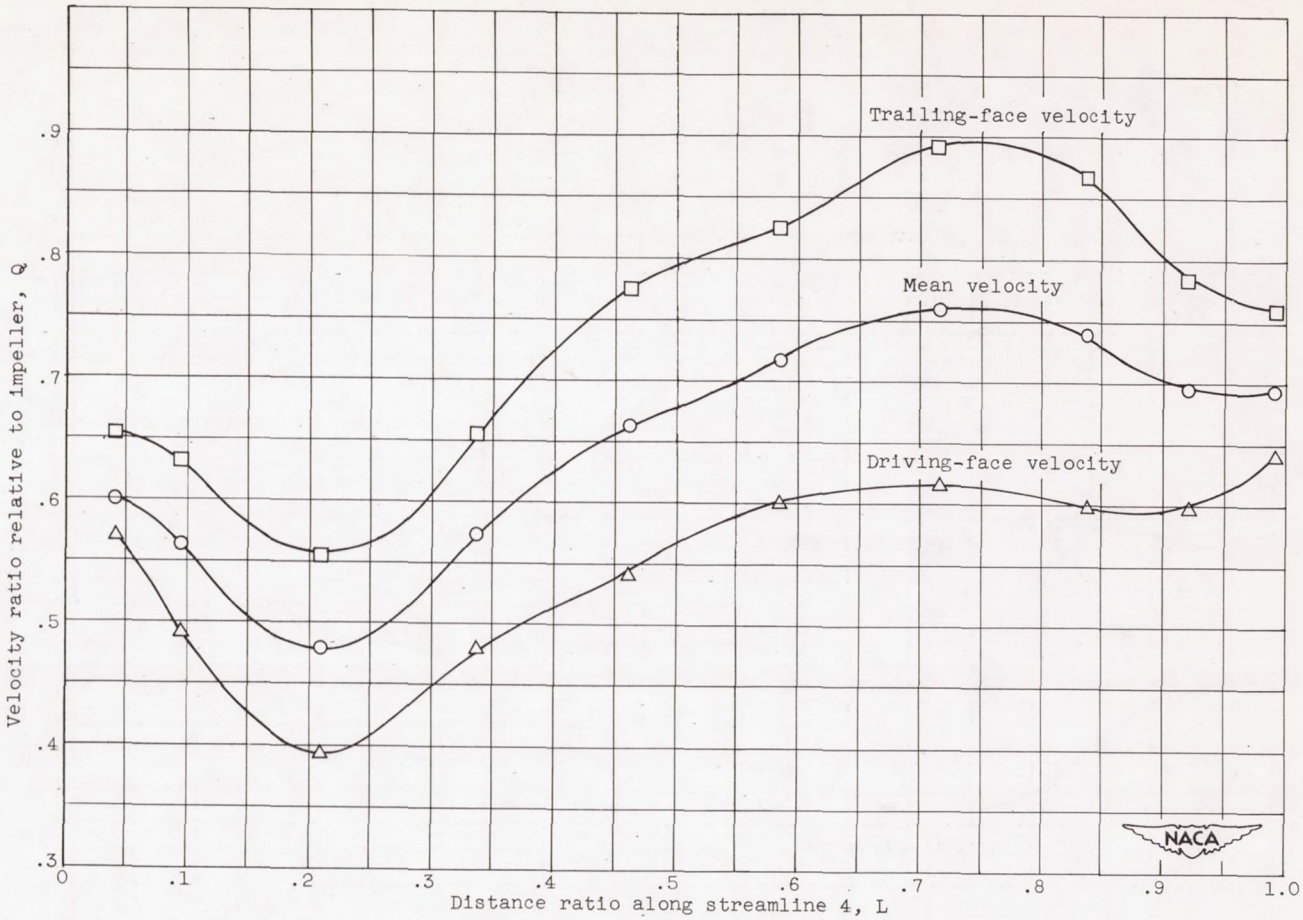

(b) Blade-to-blade velocity distribution along streamline 4.

Figure 7. - Continued. Flow analysis in blade-to-blade plane for design impeller (MFI-2). Weight flow, 13.0 pounds per second; outlet mean-line speed, 1400 feet per second.

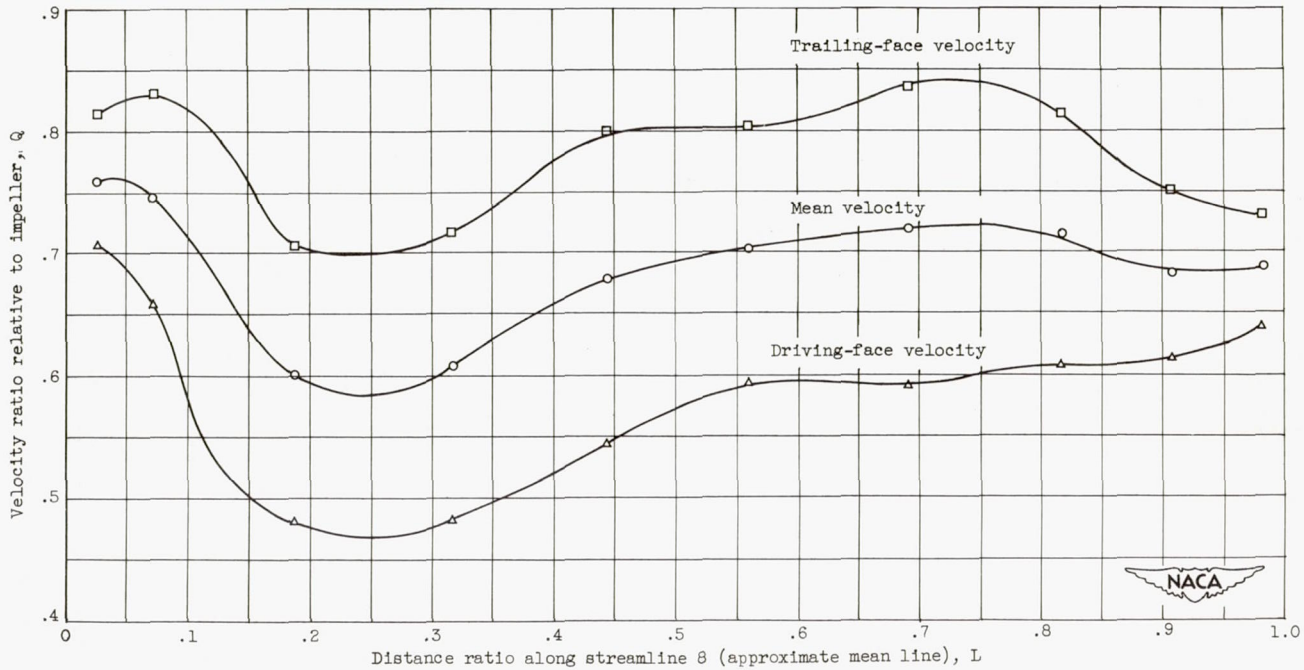

(c) Blade-to-blade velocity distribution along streamline 8.

Figure 7. - Continued. Flow analysis in blade-to-blade plane for design impeller (MFI-2). Weight flow, 13.0 pounds per second; outlet mean-line speed, 1400 feet per second.

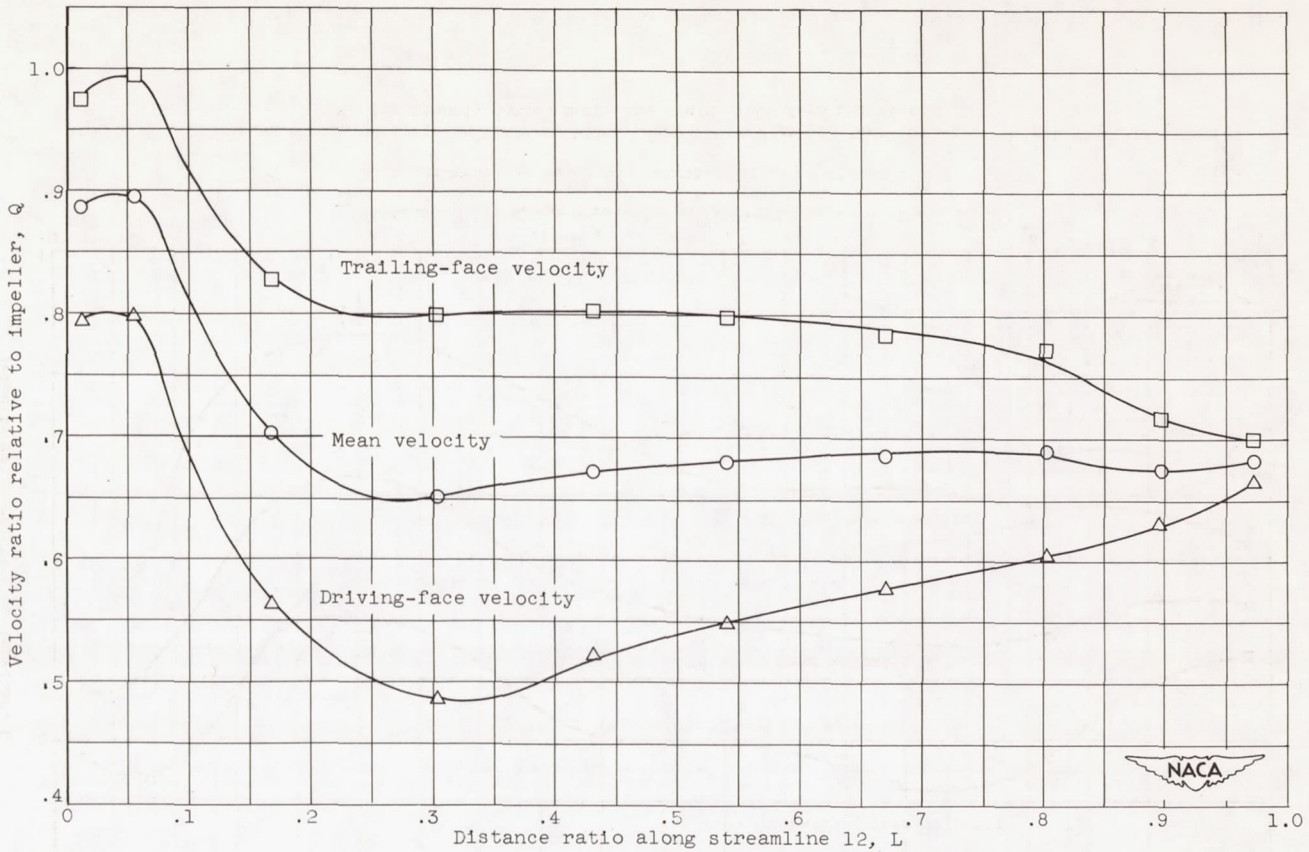

(d) Blade-to-blade velocity distribution along streamline 12.

Figure 7. - Continued. Flow analysis in blade-to-blade plane for design impeller (MFI-2). Weight flow, 13.0 pounds per second; outlet mean-line speed, 1400 feet per second.

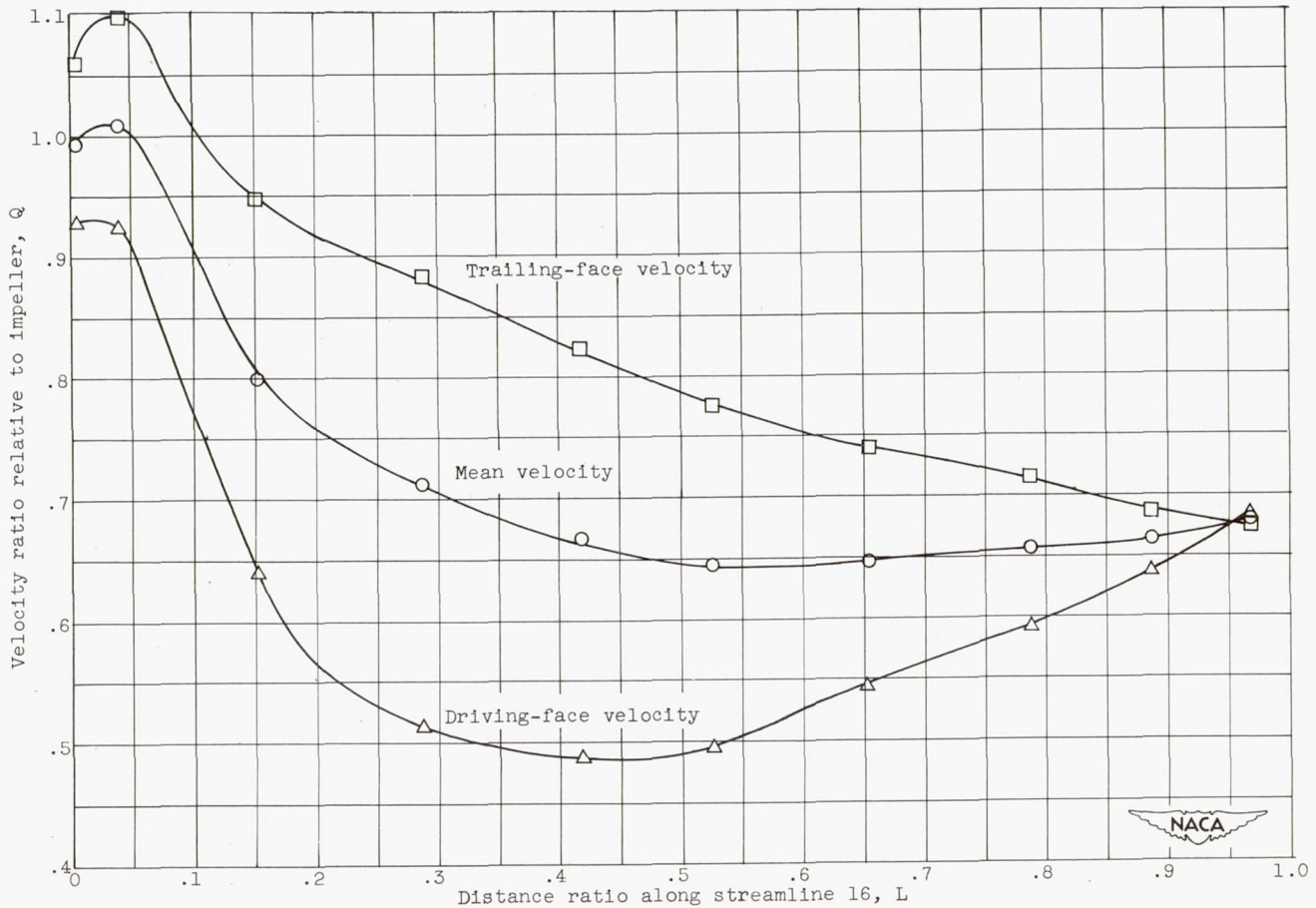

(e) Blade-to-blade velocity distribution along streamline 16.

Figure 7. - Continued. Flow analysis in blade-to-blade plane for design impeller (MFI-2). Weight flow, 13.0 pounds per second; outlet mean-line speed, 1400 feet per second.

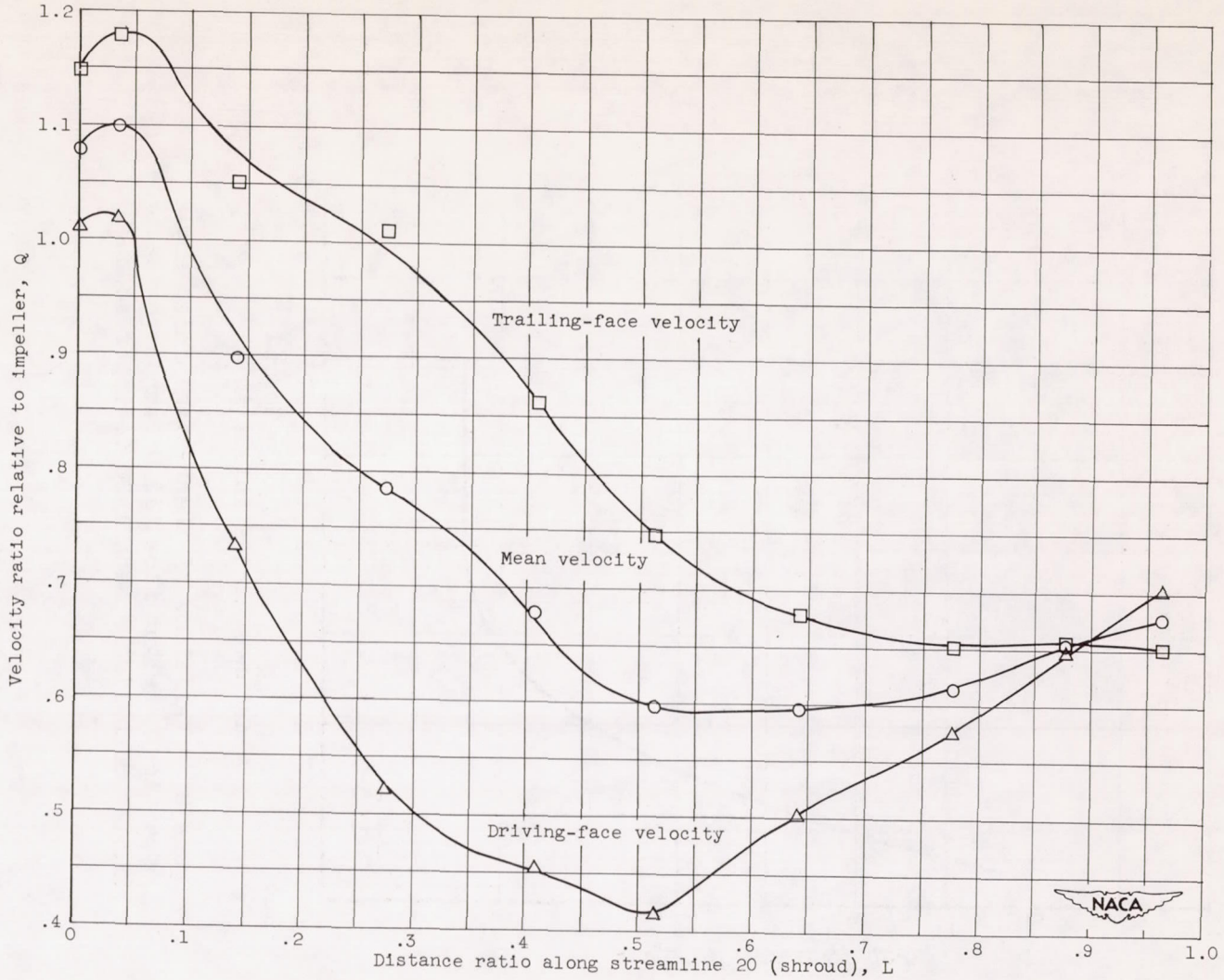

(f) Blade-to-blade velocity distribution along streamline 20 (shroud).

Figure 7. - Concluded. Flow analysis in blade-to-blade plane for design impeller (MFI-2). Weight flow, 13.0 pounds per second; outlet mean-line speed, 1400 feet per second.

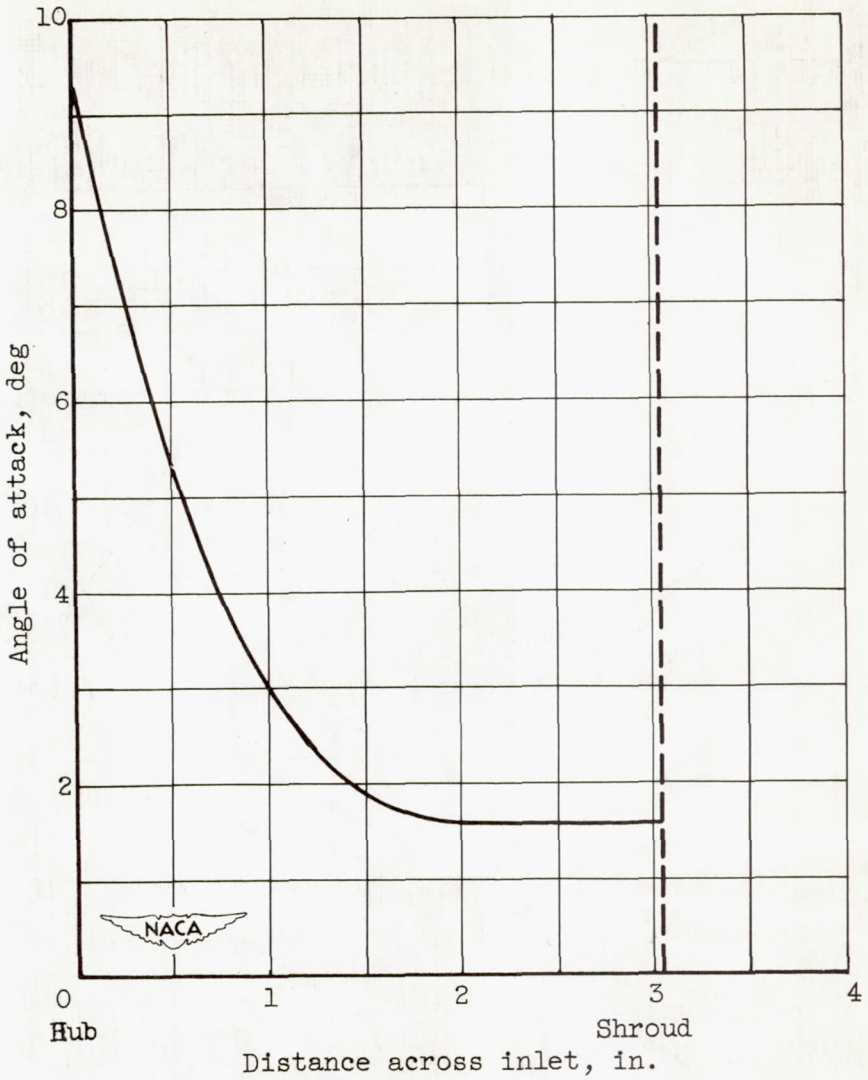

Figure 8. - Variation of theoretical inlet angle of attack. Weight flow, 13.0 pounds per second; outlet mean-line speed, 1400 feet per second.

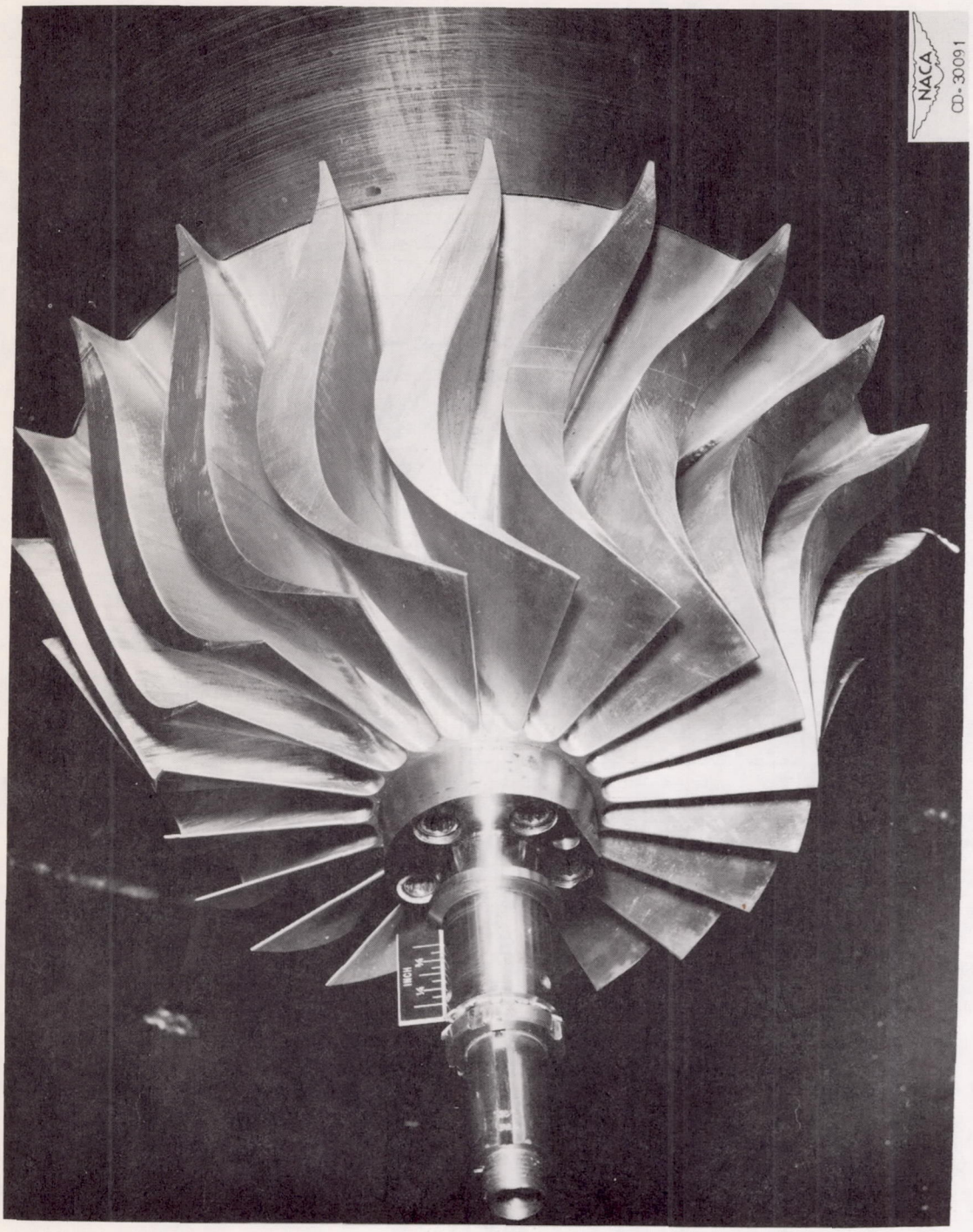

Figure 9. - Impeller model (MFI-2A).

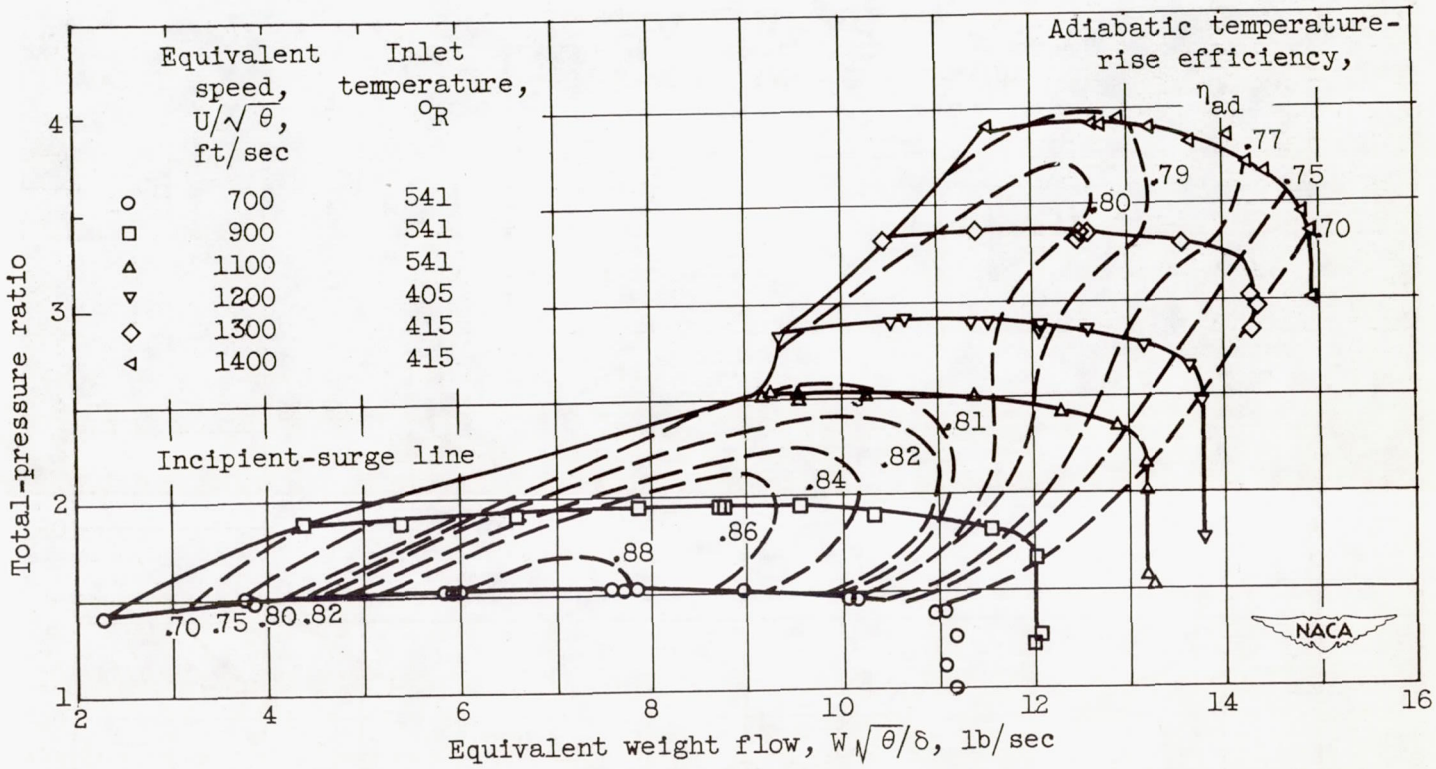

(a) Performance characteristics.

Figure 10. - Over-all performance characteristics of MFI-2A impeller at inlet-air pressure of 14 inches of mercury absolute.

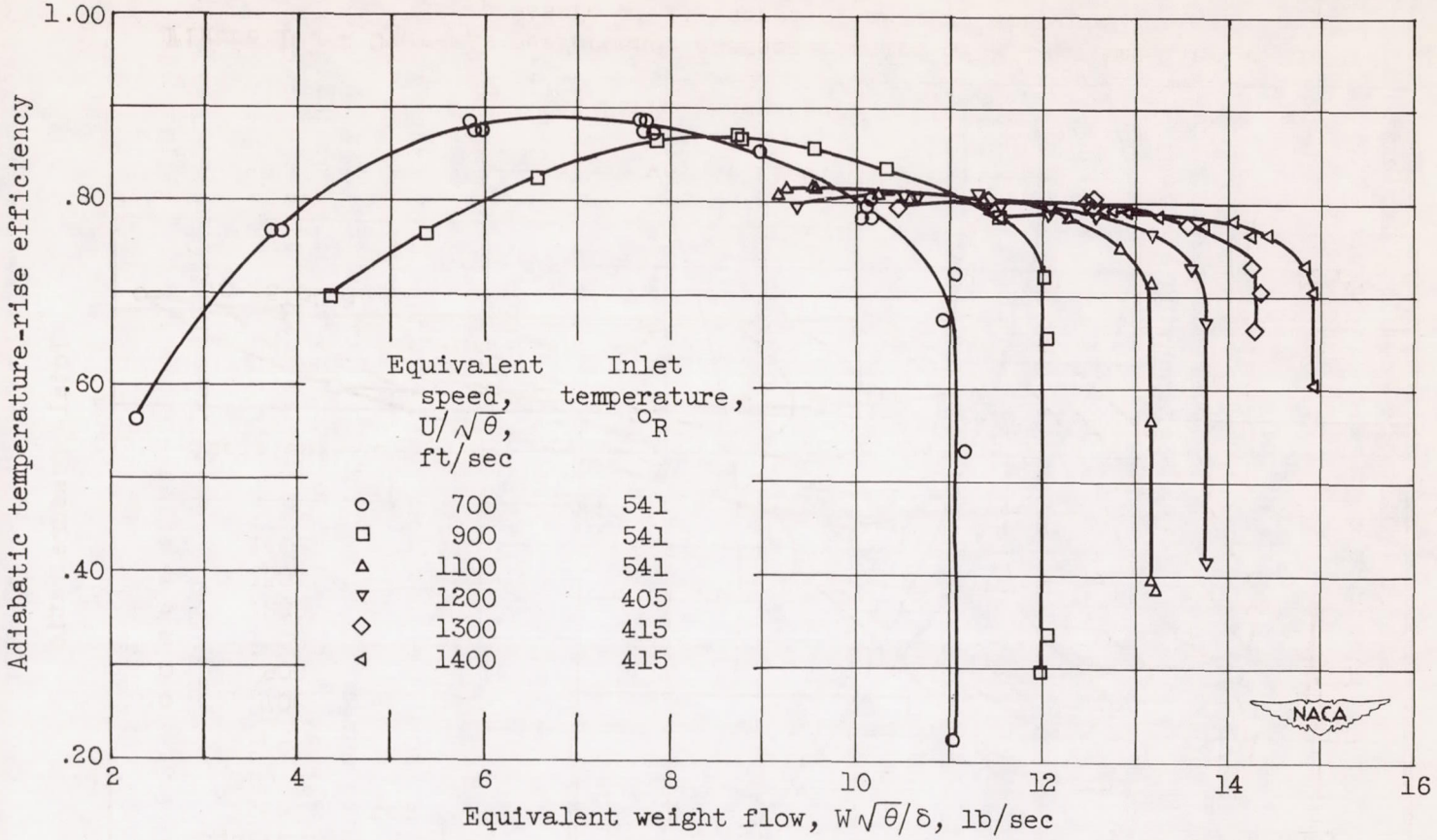

(b) Over-all efficiency.

Figure 10. - Continued. Over-all performance characteristics of MFI-2A impeller at inlet-air pressure of 14 inches of mercury absolute.

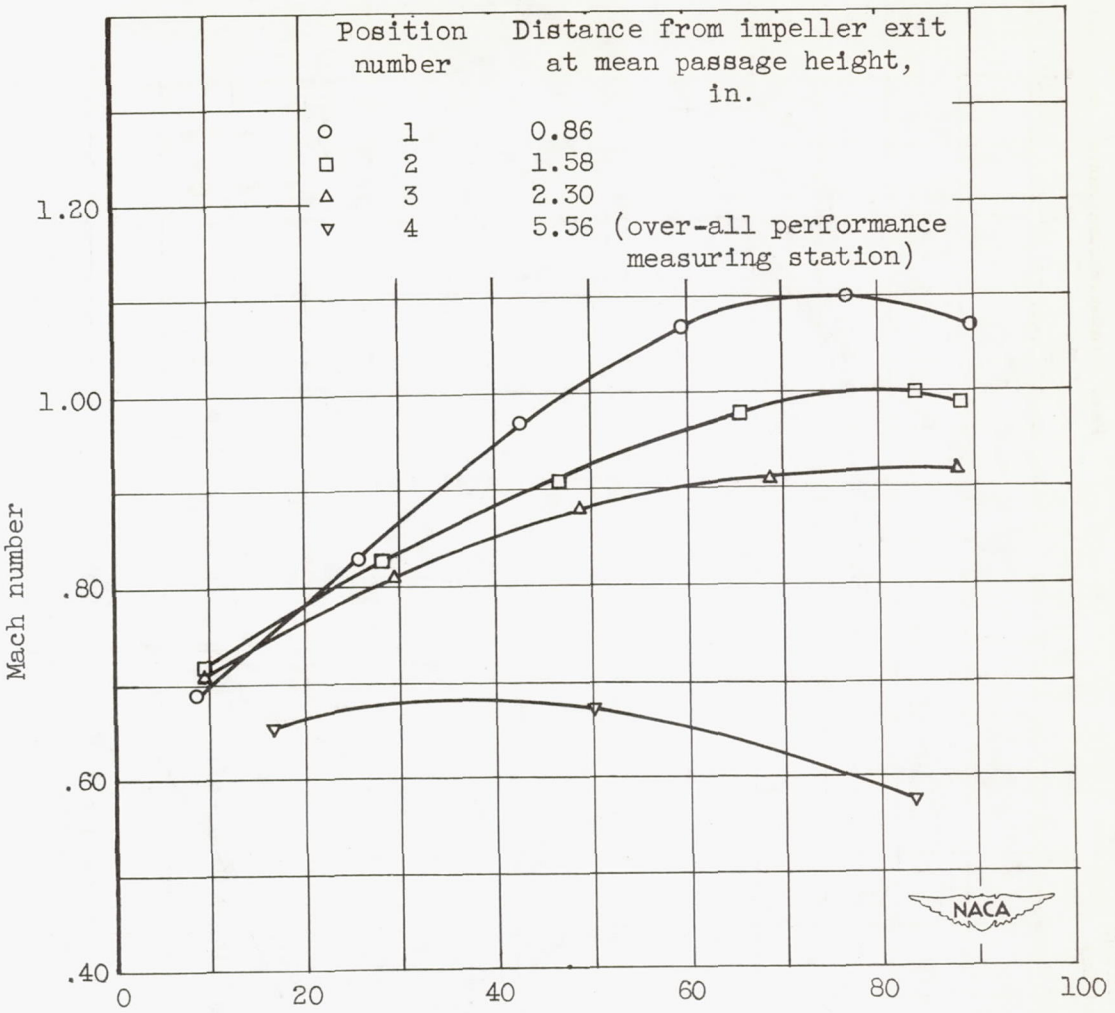

(c) Mach number at three positions across impeller exit and at over-all performance measuring station. Equivalent weight flow, 12.64 pounds per second; equivalent outlet mean-line speed, 1400 feet per second.

Figure 10. - Concluded. Over-all performance characteristics of MFI-2A impeller at inlet-air pressure of 14 inches of mercury absolute.

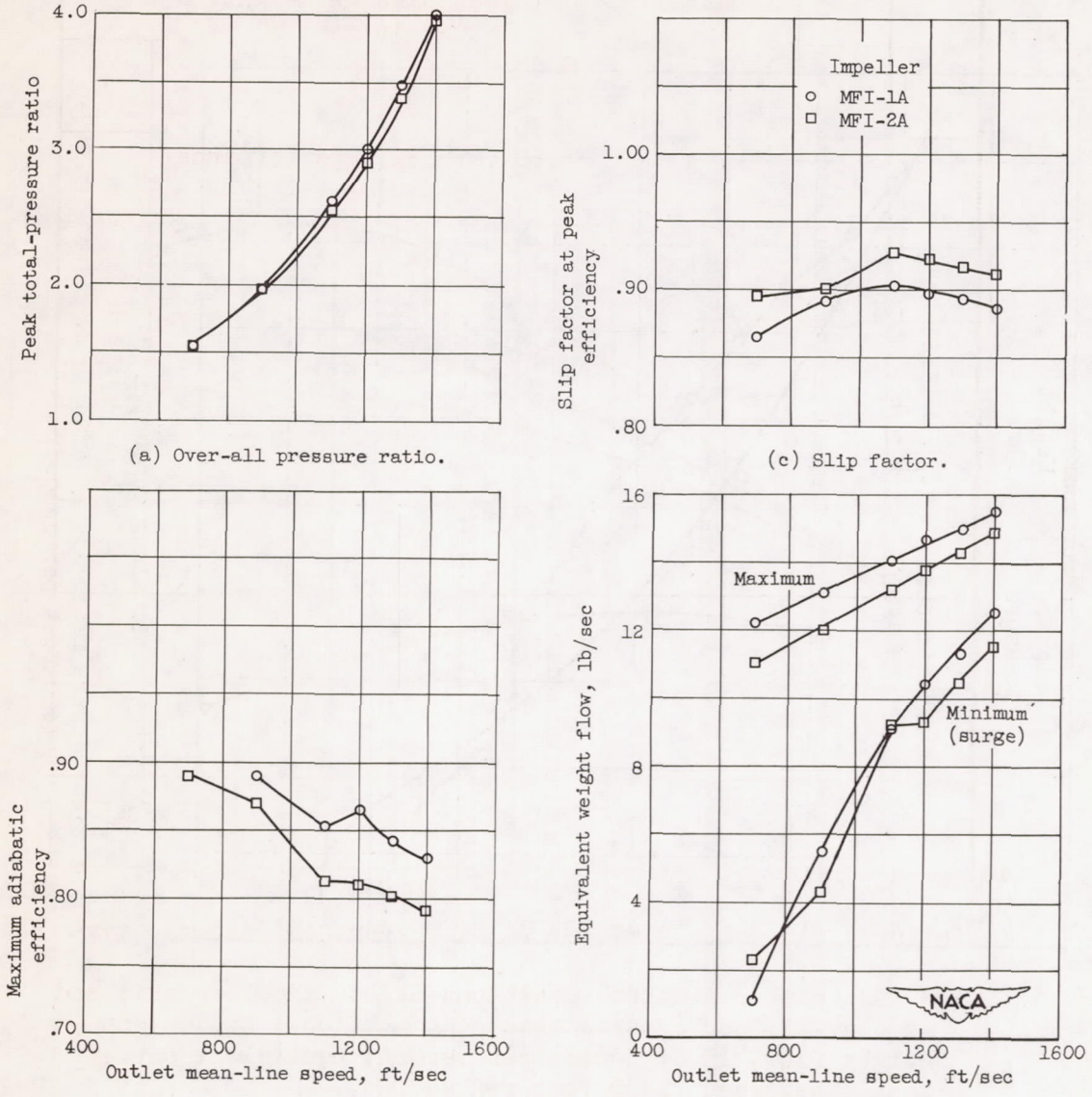

(a) Over-all pressure ratio.

(c) Slip factor.

(b) Maximum efficiency.

(d) Weight-flow range.

Figure 11. - Comparison of performance of MFI-1A and MFI-2A impellers.

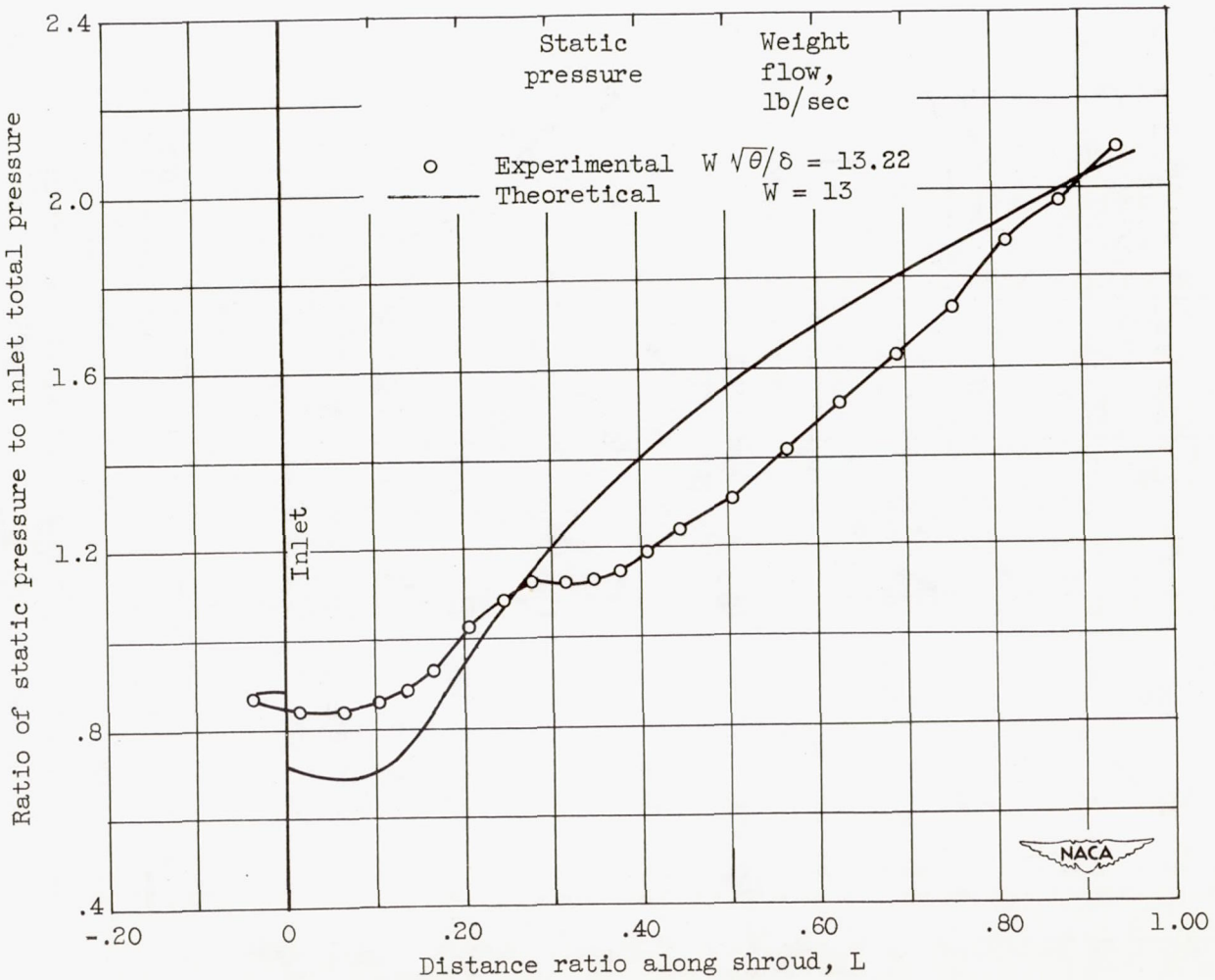

Figure 12. - Static-pressure ratio along shroud. Equivalent speed, 1400 feet per second.

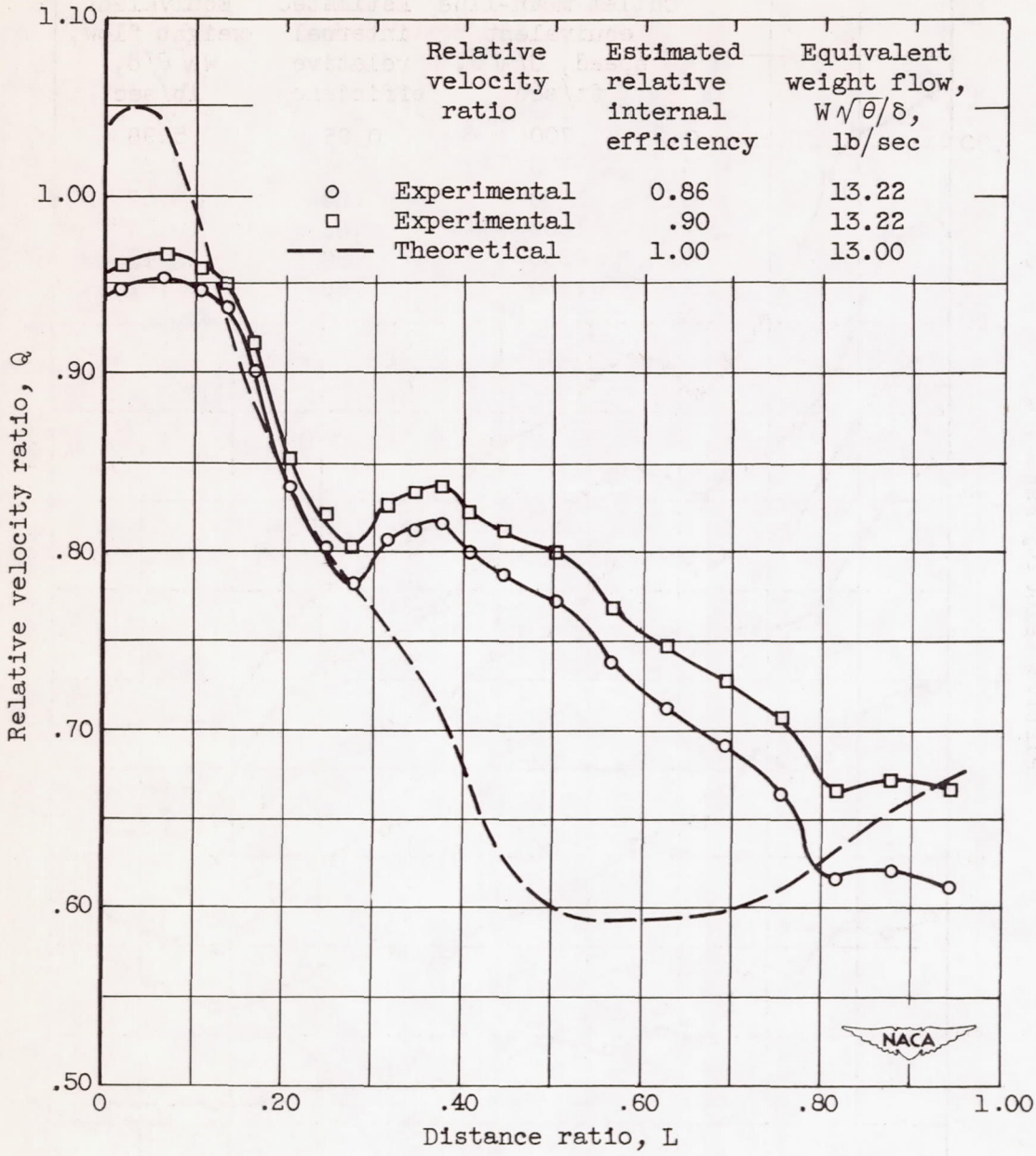

Figure 13. - Comparison of theoretical and experimental velocity ratio along shroud (MFI-2A impeller). Outlet mean-line speed, 1400 feet per second.

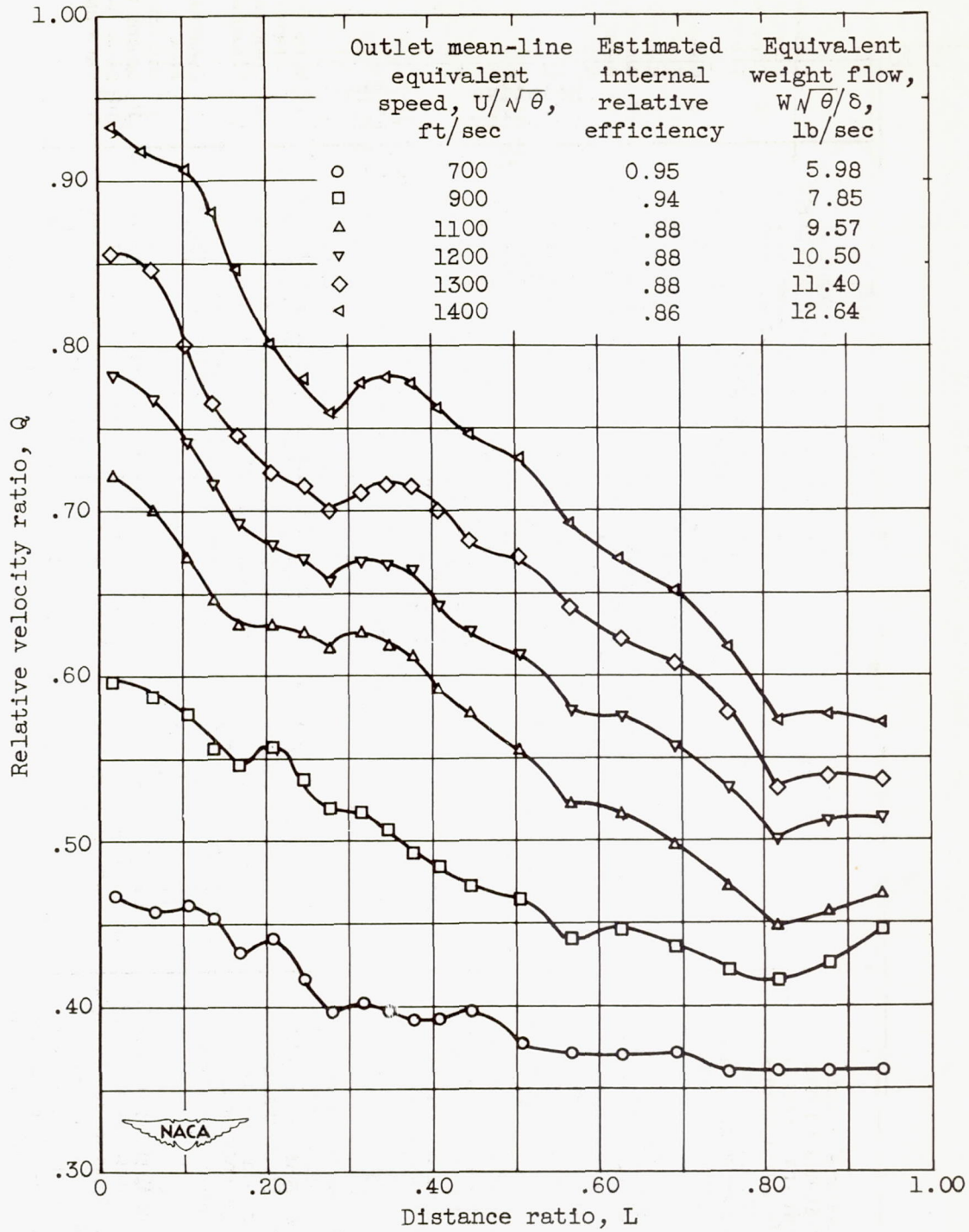

Figure 14. - Relative velocity ratio along shroud at maximum over-all efficiency and range of outlet mean-line speeds.